École polytechnique
Promotion X2015
Achille Thin

Rapport de stage de recherche
IRFM, CEA, Cadarache
Study of the WEST Tokamak at high density regimes
Rapport Non Confidentiel

Wednesday 29th August, 2018

Département de Mathématiques Appliquées
Tuteur : Hugo Bufferand
09/04/2018-10/08/2018
IRFM, Cadarache, St Paul-Lez-Durance

Déclaration d'intégrité relative au plagiat

Je, soussigné Achille Thin, certifie sur l'honneur :

1. Que les résultats décrits dans ce rapport sont l'aboutissement de mon travail.
2. Que je suis l'auteur de ce rapport.
3. Que je n'ai pas utilisé des sources ou résultats tiers sans clairement les citer et les référencer selon les règles bibliographiques préconisées.

Je déclare que ce travail ne peut pas être suspecté de plagiat.
Le 29/08/2018

Abstract

Nuclear Fusion is one of the most promising lead for a sustainable and non dangerous source of energy all around the world, in the years to come. In that regard, huge projects, such as ITER, regroup a great number of countries in order to advance hand in hand toward this solution.
However, lots of problems still exist. One of the engineering constraint on magnetic confinement is that all the particles escaping the magnetic surfaces will strike almost at the same point, the "target", which will then receive a heat flux way too important for any material known to man. Solutions must then be found to dissipate this heat before it reaches the target, without collapsing the plasma.
A particularly interesting scenario involves a high density of plasma particles, to create an ionization front detaching the target from the plasma. This can be studied with models of different complexity, which we will consider in the following. Finally, in order to validate our most complex 2D model developed by the IRFM and its results, a method to simulate a measure on the SOLEDGE2D (the program) outputs has been created and will be used at the end of this document.

La Fusion Nucléaire est une des pistes les plus prometteuses pour une source d'énergie durable et propre. Dans cette optique, d'énormes projets, tels qu'ITER, se sont lancé, sonnant une collaboration internationale pour avancer vers cette solution qu'offre la fusion.
Cependant, des gros problèmes subsistent encore. Une des contraintes d'ingénierie les plus compliquées est que les particules du plasma s'échappant de leur confinement magnétique et des surface de flux vont toutes taper quasiment au même point, la "target", qui recevra alors un flux de chaleur qu'aucun matériau connu ne peut supporter. Une solution doit donc être trouvée pour dissiper cette chaleur avant qu'elle n'atteigne la target, sans agir directement sur le plasma de coeur.
Un scénario particulièrement intéressant permettrait de créer un front d'ionisation avant les targets, les détachant ainsi du plasma, en imposant une forte densité plasma. Cela peut être utilisé avec des modèles de complexité diverses, que nous étudierons et développerons dans ce document. Enfin, pour valider le modèle 2D le plus complexe développé par l'IRFM, et ses résultats, une méthode simulant une mesure sur le programme SOLEDGE2D et ses sorties sera mise en place et utilisée.

1 Acknowledgements

I would like to thank, for their support during this internship:

- Hugo Bufferand, my tutor, and Guido Ciraolo, head of the research group, for their investment and interest in my work, as well as their support along my internship

- Julien Denis, Raffaelle Tattali, Federico Nespoli, Alberto Gallo and Matteo Valentinuzzi for their welcome in their PhD team.

- Olivier Meyer and Joël Rosato for their help with the construction and analysis of my method for synthetic diagnosis.

2 Introduction

2.1 Presentation of the Institute and Nuclear Fusion

The work presented in this document has been done during an internship at the Institut de Recherche sur la Fusion par confinement Magnétique (IRFM), an institute of the Commissariat à l'Énergie Atomique et aux Énergies Alternatives (CEA), in France. It is located at Cadarache, a research center of the CEA. CEA is a reserch center for various energies, from fossil and petrol to renewable, and nuclear fission and fusion. The last will interest us in the following.

Nuclear fusion as a source of energy has been studied for a very long time. The principal idea is to reproduce the energy source of the sun, and combine two hydrogen nucleus (deuterium and tritium) to form a Helium one. This reaction is very exothermic, but requires a great confinement of the particles for the reaction to take place.
The reaction considered is : ${}^2D + {}^3T \rightarrow {}^4He(3.5MeV) + n(14.1MeV)$.
Indeed, to overcome Coulomb electrostatic potential barrier (because the two nucleus are charged positively), they require an energy of $10keV$, so around 10^8K. However, the reaction liberates an energy of about $17.6MeV$, which gives nuclear fusion the highest ratio between energy produced and combustible mass.

Fusion is also very interesting as its fuel is almost infinite on Earth. Indeed, it uses deuterium and tritium (as they represent the couple of nucleus for which it will be the simplest), two isotopes of the hydrogen atom. Deuterium can be found as a small percentage along the hydrogen present on Earth, so in every drop of water, and its quantity is unlimited at the scale of several human lives. The tritium is rarer on Earth, however it can be produced very easily using Lithium resources, which are also numerous.

Moreover, it can be noticed that even indirectly, all of Earth sources of energy come from nuclear fusion (as they are produced by the sun) : Solar energy, wind energy (due to the irregularity of solar heat over the atmosphere), hydraulic (as the cycle of water is powered by the sun), fossil and wood energy (life is induced by the presence of the sun, and photosynthesis), and geothermal and nuclear fission (as all radioactive elements heating the mantel of the Earth or powering our nuclear plants come from heavy element fusion in the stars).

2.2 How to achieve Nuclear Fusion

A huge international cooperation project has been launched in order to develop nuclear fusion as an industrial source of energy : it is the International Thermonuclear Experimental Reactor (ITER) project, located in the center of Cadarache, France. This is the largest and most expensive international project, and its construction is planned to end in 2025, and we would then be in measure to verify the feasibility of a nuclear fusion central. However, even if we have already succeeded in creating controlled nuclear fusion reactions (in the Joint European Torus, in Oxford), it is not interesting enough yet.
Indeed, in order for the fusion to be balanced (and self sustainable), the reaction must verify the Lawson criterion : $n_i T_i \tau_e > 3 * 10^{21} m^{-3}.keV.s$ The reaction can then pro-

duce more energy than it needs to be maintained. n_i is the ionic density, T_i the ionic temperature, and τ_e the confinement time.

In the stars, such as the Sun, this confinement is obtained with gravitational forces. However, we cannot reproduce this confinement on Earth, so two solutions appears. Inertial confinement fusion and Magnetic confinement fusion. Inertial confinement uses very powerful LASERs (like the MegaJoule ray in Bordeaux), in order to reach very high ionic temperature, at the expense of the confinement time.

One other lead is magnetic confinement, which uses relative low density plasma, with a longer confinement time. The idea is the following : At the considered temperature ($10^8 K$), the matter is in the state of plasma - an ionized and charged gas. As the plasma particles are charged, one can use electric and magnetic fields to confine our combustible. A first magnetic configuration, and for now the most efficient, is the tokamak, *i.e.* a toroidal chamber with a magnetic field (Russian acronym). A central bobbin will create a toroidal magnetic field, and the movement of the plasma will induce a current that will create a poloidal field, which will roll up magnetic lines, and thus confine better the particles, according to the following graph.

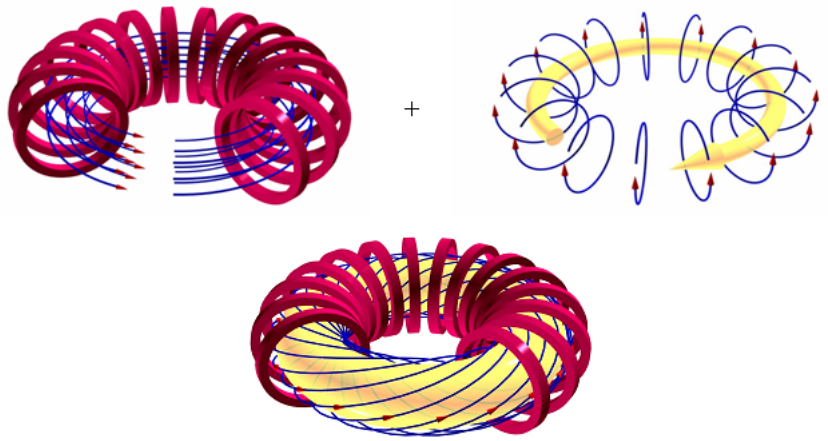

Figure 1: Magnetic configuration of a tokamak

2.3 A few issues with Magnetic confinement

In order to simplify, we will consider in the work that the particles speed is mainly parallel to the field lines, at the exception of some perpendicular transport that we will call in the following drifts.

Under that hypothesis, the plasma particles are then mainly confined in the magnetic flux surfaces (where the normal at any point of the surface is perpendicular to the local magnetic field) visible on Figure 1, as the tend to follow the magnetic lines. A poloidal cut of the tokamak would show the surfaces as presented on figure 2. We can see that the surfaces are nested and closed inside the tokamak, until they reach the separatrix, which designs the last closed flux surface. To this point, magnetic lines will

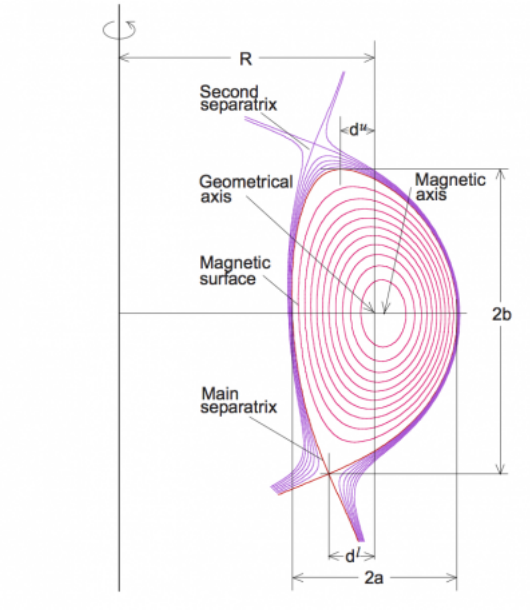

Figure 2: Magnetic configuration of a tokamak

cross the tokamak components, hitting them particularly, at the bottom of the figure, at two striking points on the piece named divertor.

The plasma outside the separatrix is called the edge plasma, or Scrape-Off Layer (SOL), and inside is called core plasma.

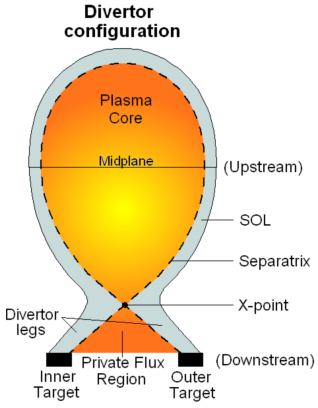

Figure 3: Divertor configuration on a poloidal cut

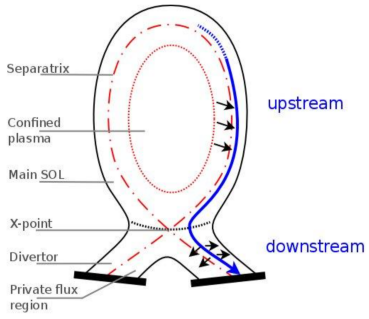

Figure 4: Particle path in a tokamak on divertor configuration

This particular piece is then the target for a very high flux of energized particles coming out of the plasma (due to drifts, and the opening of the flux surfaces at that point).

It is then a high stake engineering issue to limit the energy flux received by the divertor while still satisfying the viability of the plasma in the core region. A fusion power of $500MW$ is foreseen for ITER, and thus $100MW$ will cross the separatrix. Then, if nothing is done to reduce this flux (that is parted between a convective and a conductive flux), all the energy will go on the targets. To evaluate how the power will be dissipated at the targets, we introduce λ_q, the width of the Scrape-Off Layer. For ITER, it will be around $1mm$.

We can then compute the repartition onver the target. Indeed, the total at the divertor target considering the toroidal form is $A_{div} = 2\pi R_{div}$. Moreover, the particles do not arrive perpendicularly to the target, and [1] we have the parallel cross section which can be defined as :

$A_{\parallel} = 2 * 2\pi R_{div} \lambda_q sin(\frac{B_\theta}{B_\phi}) = 2 * 2\pi R_{div} \lambda_q \frac{B_\theta}{B_\phi}$

Thus an estimation of the parallel heat flux at the targets :

$q_{\parallel} = \frac{P_{sep}}{A_{\parallel}} = 12 \cdot 10^9 W$

In that regard, several scenarii have been considered in order to reduce that flux. The idea is to separate the targets as much as possible from the core plasma, anyway possible. A particularly interesting way of doing so, which has been a guiding line along my internship, is the detached regime.

The detached regime is a particular regime of the tokamak, characterised with a really high upstate plasma density, and a really low energy and particle flux at the target, due to a zone of recombination of the plasma in the divertor region, near the targets. A linear representation is given in figure 5.

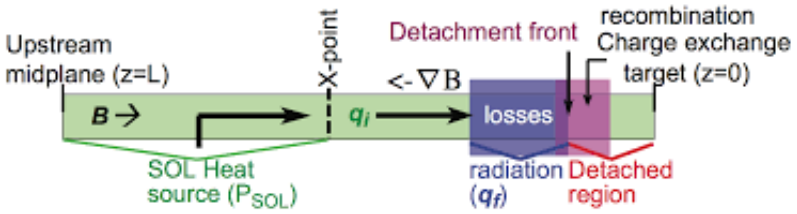

Figure 5: Linear Representation of the Detached Regime

In this particular regime, the energy flux is dissipated as it goes through a radiative zone and a recombination zone where charge exchange reactions ($H + H^+ \rightarrow H^+ + H$) and recombination are non negligible due to the low temperature. We will study this mechanism more precisely in the following part.

3 Presentation of the Equations

3.1 General Equations

In the Scrape Off Layer, to model the transport of the particles, we use the Lorentz equation :
$m\frac{\partial \vec{v}}{\partial t} = q\left\{\vec{E}(\vec{r},t) + \vec{v}\times\vec{B}\right\}$
However, the high number of particles impose us to use the probabilistic Vlasov-Landau equation, where f is the probability density function :
$\frac{\partial f}{\partial t} + \vec{v}\cdot\vec{\nabla}_x f + \frac{q}{m}(\vec{E} + \vec{v}\times\vec{B})\cdot\vec{\nabla}_v f = \left(\frac{\partial f}{\partial t}\right)_c$

The right hand side represents here all the interactions between particles (where we will intervene with well chosen closures), and sources.

However, the pure resolution of this equation is still too expensive in term of computation costs, so we have to simplify it by integrating this equation for all values for the particle velocity (it then becomes a fluid equation). We will do this manipulation in the following, expliciting the 3 first moment of the function f (by multiplying during the integration by 1, $\vec{v}$, $\frac{1}{2}v^2$). We can then define various quantities and obtain three equations.

Hypothesis In order to continue our calculus proprely, we will need proper hypothesis.

- The plasma is quasi neutral $n_i \cong n_e$
- The plasma is ambipolar $v_i \cong v_e$
- The mass of the electrons is negligible $m_e \ll m_i$

Let us define the density $n = \int f(\vec{(}v))d\vec{v}$, the velocity $\vec{u} = \frac{1}{n}\int \vec{v} f(\vec{v})d\vec{v}$.

We have then the continuity equation for moment 0 :
$\frac{\partial n}{\partial t} + \vec{\nabla}\cdot n\vec{u} = S_n$ where S_n is the source term for the particles (ionization, recombination, injection of particles, ...).

On the same way, we get the second equation :
$\frac{\partial n\vec{u}}{\partial t} + \vec{\nabla}\cdot\left(n\vec{u}\otimes\vec{u} + \frac{\mathbf{P}}{m}\right) - n\frac{\vec{F}}{m} = \vec{S}_u$

The central term comes from the second moment $\int \vec{v}\otimes\vec{v} f(\vec{v})d\vec{v}$ which can be simplified using $\vec{v} = \vec{u} + \vec{v'}$, where $\vec{u}$ is the mean velocity, and $\mathbf{P} = m\int \vec{v'}\otimes\vec{v'} f(\vec{v})d\vec{v}$ where the isotropic pressure can be defined as $p = Tr(\mathbf{P})/3$.

We can then define the total energy as a sum of a macroscopic and a microscopic contribution :
$E_t = \frac{1}{2}mnu^2 + \frac{3}{2}p$
Let us denote as $\vec{Q} = \frac{nm}{2}\int \vec{v'}\vec{v'}^2 f(\vec{v})d\vec{v}$ the conductive flux, and $\mathbf{P} = 3p + \Pi$, Π being the viscosity tensor.

The third equation is then the following :
$\frac{\partial \frac{nm}{2}\vec{u}^2 + \frac{3p}{2}}{\partial t} + \vec{\nabla}\cdot\left((\frac{nm}{2}\vec{u}^2 + \frac{5p}{2} + \Pi)\vec{u} + \vec{Q}\right) = nq\vec{E}\cdot\vec{u} + S_E$

In the following, we will always assume $p = k_b nT$, and in order to close these equations, we have to make an assumption about the condutive flux (the highest moment).

3.2 Closure

The closure will be the following, according to a well known law for ions and electrons :

$Q_{e,i} = -K_{e,i}\vec{\nabla}T_{e,i}$, with $K_{e,i} = K_{0e,i}T_{e,i}^{5/2}$

3.3 Bohm Boundary Conditions

Near the wall, physics is quite different as some kind of sheath forms and modifies the local behaviour of magnetic and electric field. However, conditions at the entrance of this sheath have been found, and allow us to extend our model to the wall.

Indeed, the velocity of the ions and the electrons at the entrance of the sheath can then be compared to the local sound speed :

$v \geq c_s$ where $c_s = \sqrt{\frac{k_b(T_e+\gamma T_i)}{m_i}}$ where γ is a polytropic index, depending on the regime.

Moreover, the heat fluxes can be known too :

$q_{e,i} = \gamma_{e,i}T_{e,i}\Gamma$ with $\Gamma = nv$ the particle flux at the entrance of the sheath.

4 The Two-Points Model

As the codes to model 2D or 3D plasma are very expensive in computation costs, it is interesting to build a very simple model, easy to analyze and allowing a good prediction of the tendency of the plasma behavior, putting forward different working regimes in the Scrape Off Layer.

4.1 Presentation of the Two Points Model

This model, as its name indicates, does not try to model a whole surface of flux, or a simple line, but only two points : Upstream, and downstream (at the target).
In that regard, it can be qualified as a 0D model.

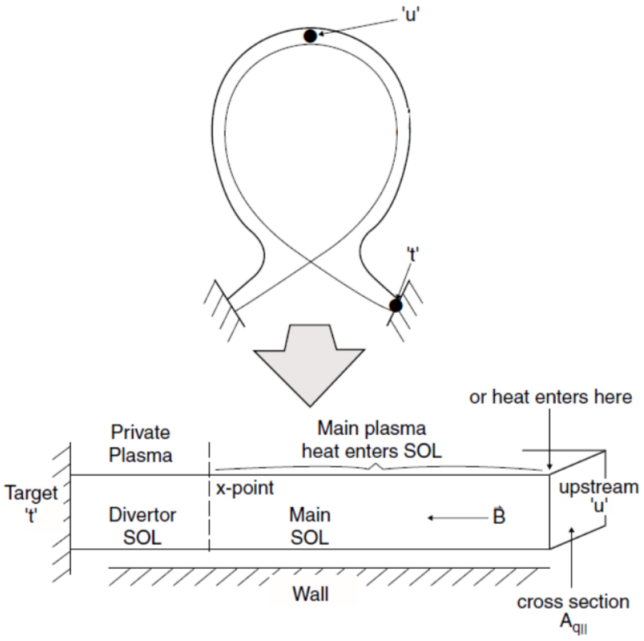

Figure 6: Representation of the Two-Point Model

It takes as arguments only the upstream density, and the power coming in the Scrape Off Layer P_{sep}, and computes at the target the density, the particle and energy flux, and the temperature upstream and downstream. It uses as parameters the length of a magnetic line L (connection length), the parallel cross section, and the percentage of impurity.

One important assumption is here $T_i = T_e$, and the Bohm inequalities are here equalities.

At its simplest version, the hypothesis are very strong, but it can be possible to refine it a bit.

4.2 Basic Two Points Model

For the basic Two Points Model, no pressure losses are considered, and the heat flux is considered to be conductive at a constant f_{cond} rate, only directed along the magnetic line, as well as electron and ion velocities. As we have the initial condition upstream : $v = 0$ by symmetry, we have the following equations :
$k_{0,e} T^{5/2} \frac{dT}{ds} = f_{cond} q_{\parallel}$ with $q_{\parallel} = \frac{P_{sep}}{A_{\parallel}}$ the parallel heat flux, so $T_u^{7/2} = T_t^{7/2} - \frac{7 L f_{cond} q_{\parallel}}{2 k_{0,e}}$
$q_{\parallel} = \gamma k_b T_t \Gamma_t$ at the target according to Bohm condition
$n_u T_u = n_t T_t + n_t m c_s = 2 n_t T_t$
$\Gamma_t = n_t \sqrt{\frac{k_b T_t}{m_i}}$ We can then compute the following graphs, with the values $P_{sep} = 2.5MW$, and n_u in abscissa.

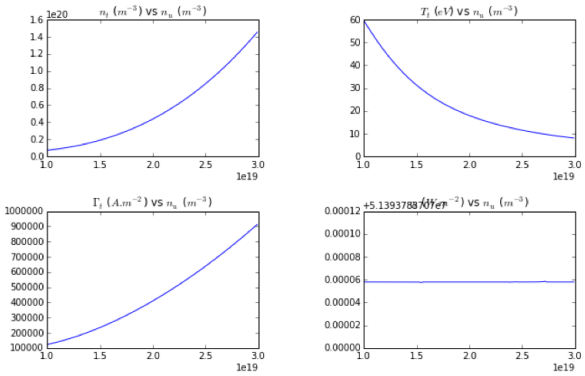

Figure 7: Graph for the Basic Two Points Model

We can see no clear change in the different functioning regime at the target. It is sign that our model is not complete enough, and we will add corrective factors to understand better, as presented in [4]

4.3 Refined Two Points Model

The first hypothesis being too strong, we will now add to our model two corrective factors, modelling the actions of the neutrals and the impurities, dissipating energy around the target, and at the origin of the different functioning regimes.

First, let us consider the radiative loss function. Following [3], we suppose:
$q_rad = \frac{14}{3} L c_z n_u^2 L_z$ where L_z is the radiative power coefficient presented in the figure 8.

Moreover, one important parameter to take into account are pressure losses. They can be model as follow [5] /
$2 n_t T_t = f_{mom} n_u T_u$ with $fmom = 2(\frac{\alpha}{\alpha+1})^{\frac{\alpha+1}{2}}$, $\alpha = \frac{<\sigma v>_{iz}}{<\sigma v>_{iz} + <\sigma v>_{cx}}$, $< \sigma v >_{iz,cx}$ being the reaction rates associated with ionization and charge exchange. f_{mom} is also presented

on figure 8. The equations become then

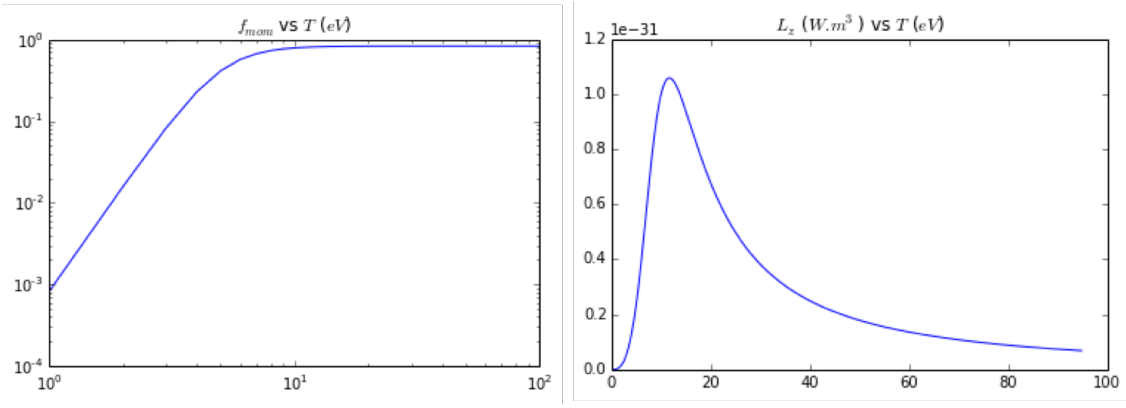

Figure 8: Correction factors for the refined Two Points Model

$T_u^{7/2} = T_t^{7/2} - \frac{7Lf_{cond}q_{\|}}{2k_{0,e}}$
$q_{\|} = \gamma k_b T_t \Gamma_t + q_{neut} + q_{rad}$ at the target according to Bohm condition
$q_{neut} = \gamma c_s (\frac{n_u T_u}{2} - n_t T_t)$
$f_momn_u T_u = 2n_t T_t$
$\Gamma_t = n_t \sqrt{\frac{k_b T_t}{m_i}}$
and the graph become then, under the same conditions :

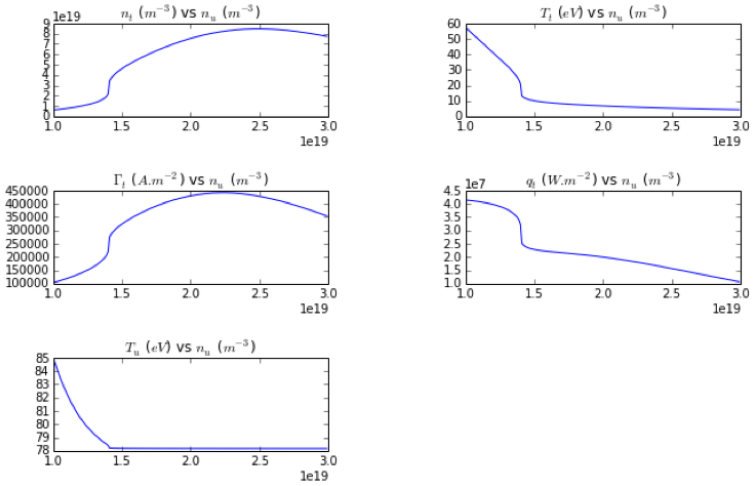

Figure 9: Graph for the Refined Two Points Model

We can the see a clear change in the regime of the target. For an upstream density under $1.5 \cdot 10^{19} m^{-3}$, the plasma is said attached, then until $1.7 \cdot 10^{19} m^{-3}$, it is the high

recycling regime, partially detached and the detached after $2.1 \cdot 10^{19} m^{-3}$.

5 1D model

In order to palliate the Two Points Model limits, we wanted to compute a 1D model of our plasma.

Indeed, the idea was to consider the characteristics of the plasma along the separatrix, using equations enhancing the neutrals roles (as we saw their importance in the Two Points Model), and to put forward the presence of an ionization/recombination front before reaching the target in the detached regime, helping then a lot for the analysis for the much more complex 2D simulations.

The set of equation was the following :

$\frac{\partial n}{\partial t} + \vec{\nabla} \cdot n\vec{u} = nn_n < \sigma v >_{iz} - n^2 < \sigma v >_{rec}$

$\frac{\partial nv}{\partial t} + \vec{\nabla} \cdot (mnv^2\vec{b}) = -\nabla_{\parallel} p + nn_n v_n < \sigma v >_{iz} - n^2 v < \sigma v >_{rec} - nn_n v < \sigma v >_{cx}$

$\frac{\partial \frac{3nT_i + mnv^2}{2}}{\partial t} + \vec{\nabla} \cdot (\frac{5nT_i v}{2}\vec{b} + \frac{mnv^3}{2}\vec{b} - K_i \nabla_{\parallel} T_i \vec{b}) = envE_{\parallel} - \frac{3n}{2\tau_{ei}}(T_i - T_e) + nn_n E_n < \sigma v >_{iz}$
$- n^2 E_i < \sigma v >_{rec} - nn_n v^2 < \sigma v >_{cx}$

$\frac{\partial \frac{3nT_e}{2}}{\partial t} + \vec{\nabla} \cdot (\frac{5nT_e v}{2}\vec{b} + K_e \nabla_{\parallel} T_e \vec{b}) = -envE_{\parallel} + \frac{3n}{2\tau_{ei}}(T_i - T_e) + -n^2 E_e < \sigma v >_{rec}$

With Bohm boundary conditions.

Those equations a substantially the ones presented above, with the source terms fixed at the ionization and recombination rates, along with pressure losses with charge exchange.

I tried to find an analytical solution, with simplified equations, and a numerical one with those real ones, but I did not get the time to finish either.

6 Synthetic Diagnosis and Relation Simulation/Experience

We are now considering a synthetic diagnosis on Visible Spectroscopy.

Visible spectroscopy is used in the WEST tokamak in order to retrieve data from experience and to compare it to simulation. The multitude of spectroscopes which can be tuned on different frequencies can estimate various parameters of the plasma itself or impurities as Tungsten [1]. Moreover, the study of Visible spectroscopy is very useful to detect detachment, as the emission of the Balmer series of the Hydrogen atom is very fluctuant around $1 - 10eV$, which is exactly the range of temperature that we expect near a detached plasma.

We center the experimental spectroscopes on the D_α ray and compare the signal received with the synthetic measure obtained according the following protocol. We use SOLEDGE2D and EIRENE [6] results to compute local plasma characteristics along the spectroscope line. Using a program from Joël Rosato [2], we obtain a normalized profile for a Stark-Zeeman D_α ray (using electronic temperature and density, and magnetic field and its angle with the line of sight).

Stark effect is a broadening of a spectral line due to the electric field, caused here in the plasma by the generation of micro-electronic fields (thus the dependency in electronic density and temperature). However it will not be much relevant here, as it is negligible for the first rays of Balmer series compared to Doppler broadening for the temperatures considered.

Zeeman effect is the splitting of an atom energy levels due to the presence of a magnetic field (the coupling of the atom's magnetic moment with the magnetic field adds a term in the hamiltonian of the system).

That profile is then convolved with a shifted maxwellian modeling neutrals speed distribution along the line of sight (considering the neutrals at a local thermodynamic equilibrium), and multiplied by the theoretical intensity of the ray (calculated supposing thermodynamic equilibrium). All the local profiles are then integrated to compute the final signal, supposed to be received by the spectroscope. Those models can be discussed, but their relevant results are presented after.

In the following, two sets of results of SOLEDGE2D will be considered, one with Oxygen as an impurity, the other with Argon.

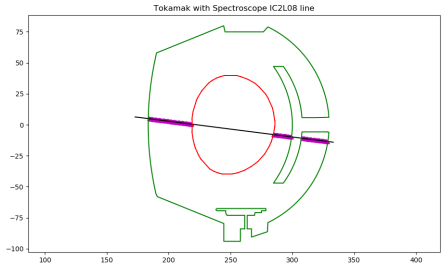

Figure 10: Spectroscope line represented on a poloidal section of WEST

The previous figure represents the line of sight of the spectroscope we consider here. The purple dots are the points on which we calculate a local profile for D_α ray emission - the temperature in the core is sufficiently high to neglect this particular emission, and the focus will be then on SOLEDGE2D results.

For a given plasma shock, we can then compare experimental and simulated results to define the pertinence of the simulation. Plotting the different characteristics relevant to our signal, we can also analyze the profile obtained. We consider here two simulations, one with Oxygen impurity, the other with Argon impurity. On both those simulations, EIRENE temperature for neutrals is slightly larger than expected - and Doppler broadening is then more important than Zeeman effect and we only observe one peek, which is contradictory with experimental results. We will then consider two other cases, with the temperature of the neutrals forced at $2eV$ (coherent with the energy of dissociation of D_2) and with the temperature only divided by a factor 2 (which brings wall neutrals energy at $2eV$ again). We will justify those modifications in the following.

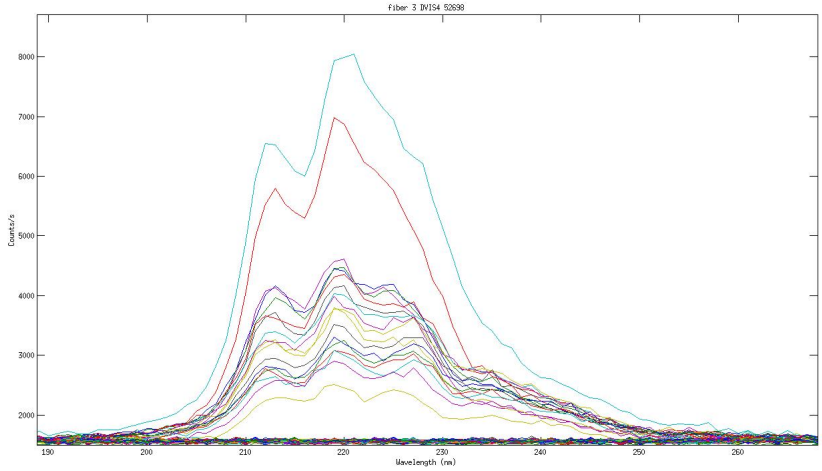

Figure 11: Experimental Signal

The two outliers signal will not be considered here, as the focus will be on the three peaked signals, much more numerous.

Indeed, we will study the averaged signal over the whole flat top phase, in order to reduce at best the noise of our measure.

The several peaks on this image are due to Zeeman effect, combined with a Doppler shift, as we will show in the simulations. However, the neutrals temperature to achieve such a precision between the peaks must go below $3eV$: The Zeeman effect splits the energy levels of the neutrals D, adding $\pm\vec{\mu_B}\cdot\vec{B}$ to the transition energy (μ_B being here Bohr's magneton). In order to see the triplet, the temperature of the neutrals must be below this energy, else the Doppler broadening absorbs it. That can be observed

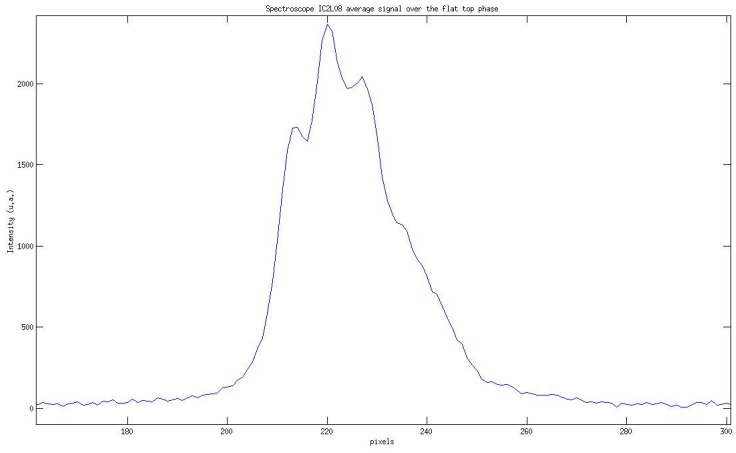

Figure 12: Experimental Signal averaged over the flat top phase

in the following figures, where neutrals temperatures reaches only $5eV$ at the least, as presented below (s is here the curvilinear abscissa, the origin being the point with minimal radius from the axis of the torus, *i.e.* at the left on the poloidal section of the tokamak presented earlier).

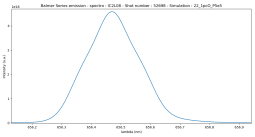

Figure 13: D_α ray for the Oxygen simulation

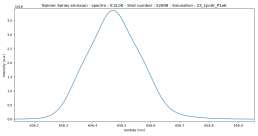

Figure 14: D_α ray for the Argon simulation

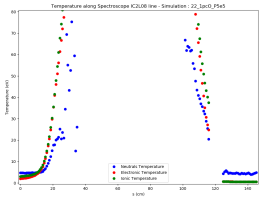

Figure 15: EIRENE results for Neutrals Temperature for the Oxygen simulation

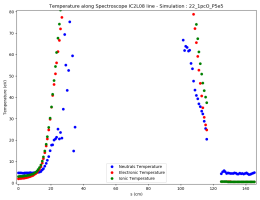

Figure 16: EIRENE results for Neutrals Temperature for the Argon simulation

Thus, we will modify EIRENE output to make sure that this condition is respected.

This will happen two separate ways. We will then divide EIRENE output for temperature by a factor 2 to reach near the wall a temperature of roughly $2.3eV$, energy of a deuterium atom after a Franck-Condon dissociation of D_2.

Those assumptions can be sustained by the following graphs, representing the importance of each point in the final graph.

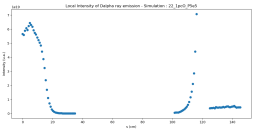

Figure 17: Local D_α ray Intensity for the Oxygen simulation

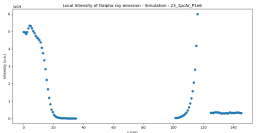

Figure 18: Local D_α ray Intensity for the Argon simulation

These graphs show that the most radiant points for this ray are almost exclusively the nearest to the walls of the tokamak. The most important neutral source being the recycling, and particularly the reaction $D_2 + e \rightarrow D + D + e$, giving a total amount to the two deuterium atoms $4.52eV$, *i.e.* roughly 2 or $2.5eV$ each.

Modifying EIRENE temperature by diving it by a factor 2, we obtain the following graph for temperature :

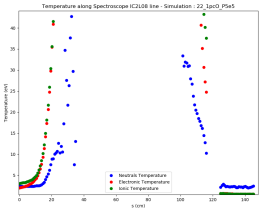

Figure 19: Corrected Neutrals Temperature for the Oxygen Simulation

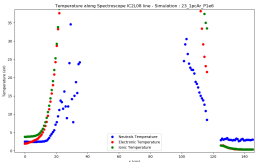

Figure 20: Corrected Neutrals Temperature for the Argon simulation

For these lower temperatures, the profiles are:

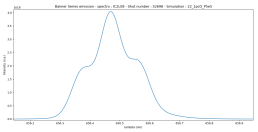

Figure 21: D_α ray for the Oxygen simulation - corrected temperature

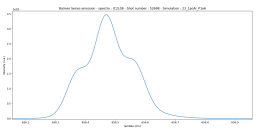

Figure 22: D_α ray for the Argon simulation - corrected temperature

Those profiles are much nearer to the experimental signal than previously: Three peaks are visible on those profile, the two on the sides being less intense than the central

one. Moreover, the spreading at the right end of the signal is also present. Finally, the signal is spread over 5.5$\AA$ (from 6562.5$\AA$ to 656.8$\AA$, and the pixel resolution for the experimental signal is approximately $0.117\AA/p$ around 656nm. The signal spreading over 50$pixels$, it is 5.85$\AA$ wide. The two signals are then really close, except for the global intensity of the peaks which can be controverted by the very strong assumption of thermodynamic equilibrium for the calculation of the local intensity (a collisional radiative model is studied for a better modeling).

The presence of the three peaks is completely explained by the Zeeman effect, centered around D_α vacuum wavelength. Neutral speed along spectroscope line cause

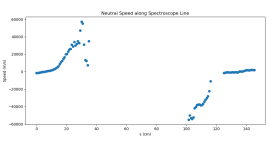

Figure 23: Neutral speed along spectroscope line for the Oxygen Simulation

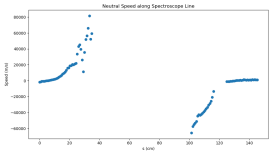

Figure 24: Neutral speed along spectroscope line for the Argon Simulation

however a Doppler shift on the D_α emission, especially at the outer wall, where there is a smaller emission, but an important speed of the neutrals. The calculation of the ray with this Doppler effect entails a shift to the left of the wavelength spectrum, causing the left peak to be slightly more important than the right one, and the spreading at the right end on the signal. Without a really precise calibration of the spectroscope, it is however impossible to compare the absolute wavelength of the signal received. This synthetic diagnosis shows then a really good accordance between simulation and experience. Even if the signals cannot be compared absolutely, their respective broadening is the same, and the different relative specificities of the measured signal can be explained and interpreted using the synthetic diagnosis and the plasma characteristics computed in the simulation.

7 Conclusion

The work conducted in this internship was under the general theme of the study of the detachment regime. In that sense, a first approach was made using a simple yet significant Two-Point Model, allowing a fast and easy computation of the general functioning regime of a tokamak under a certain set of parameters.

An advance possible on this model would be a 1D model, computing more precise results yet on a simpler way considering the alternative 2D and 3D codes. A 1D model was proposed and considered, but lacked time to succeed in giving satisfying results.

Finally, an important part of the job was developing that synthetic diagnosis tool for Visible Spectroscopy, furnishing a powerful way to compare simply and relevantly simulation and experience.

References

[1] Meyer,O. and Giacalone,J. C. and Gouin,A. and Pascal,J. Y. and Klepper,C. C. and Fedorczak,N. and Lotte,Ph. and Unterberg,E. A. and Fehling,D. T. and Harris,J. H. *Visible spectroscopy diagnostics for tungsten source assessment in the WEST tokamak: First measurements* Review of Scientific Instruments, 2018

[2] J. Rosato and Y. Marandet and R. Stamm *A new table of Balmer line shapes for the diagnostic of magnetic fusion plasmas* Journal of Quantitative Spectroscopy and Radiative Transfer, 2017

[3] C.S.Pitcher and P.C.Stangeby, Plasma Phys. Control. Fusion 39 (1997) 779–930

[4] Davide Galassi, Domiziano Mostacci, Hugo Bufferand, Guido Ciraolo, *Investigating heat flux imbalance in the complex geometries of fusion devices and assessing simplified models as guide lines to code understanding and pre-design tools for reactors*, Tesi di Laurea, 2013

[5] Christophe Guillemaut, *Modélisation du bord d'un plasma de fusion en vue d'ITER et validation expérimentale sur JET*, PhD in Physics, 2013

[6] H. Bufferand and C. Baudoin and J. Bucalossi and G. Ciraolo and J. Denis and N. Fedorczak and D. Galassi and Ph. Ghendrih and R. Leybros and Y. Marandet and N. Mellet and J. Morales and N. Nace and E. Serre and P. Tamain and M. Valentinuzzi *Implementation of drift velocities and currents in SOLEDGE2D–EIRENE*, Nuclear Materials and Energy, 2017